IEEE Photonics Journal
An IEEE Photonics Society Publication

Open Access

Investigation on Three-Hump Phosphor-Coated White Light-Emitting Diodes for Healthy Lighting by Genetic Algorithm

Volume 11, Number 1, February 2019

Ziquan Guo
Kai Liu
Lili Zheng
Tien-mo Shih
Yijun Lu
Tingzhu Wu
Yi Lin
Yuxue Zhang
Jianghui Zheng
Jie Chen
Lianxin Chen
Zhong Chen

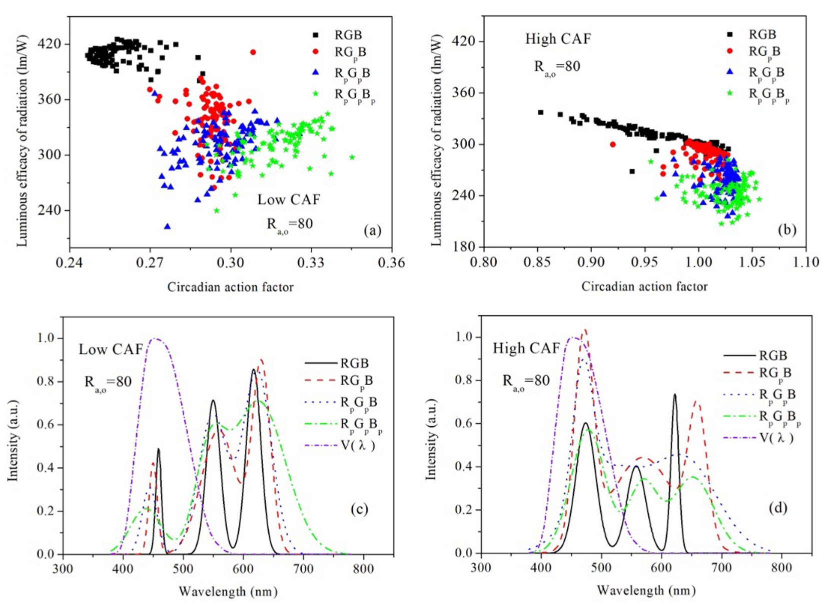

DOI: 10.1109/JPHOT.2018.2885091
1943-0655

Investigation on Three-Hump Phosphor-Coated White Light-Emitting Diodes for Healthy Lighting by Genetic Algorithm

Ziquan Guo,[1] **Kai Liu**,[1] **Lili Zheng**,[1] **Tien-mo Shih**,[1] **Yijun Lu**,[1] **Tingzhu Wu**,[1] **Yi Lin**,[1] **Yuxue Zhang**,[1] **Jianghui Zheng**,[2] **Jie Chen**,[3] **Lianxin Chen**,[3] **and Zhong Chen**[1]

[1]Department of Electronic Science, Fujian Research Center for Solid-State Lighting, Xiamen University, Xiamen 361005, China
[2]School of Photovoltaic and Renewable Energy Engineering, University of New South Wales, Sydney, NSW 2052, Australia
[3]Xiamen Hualian Electronics Corporation, Ltd., Xiamen 361006, China

DOI:10.1109/JPHOT.2018.2885091

Manuscript received November 9, 2018; revised November 27, 2018; accepted December 1, 2018. Date of publication December 7, 2018; date of current version January 1, 2019. This work was supported in part by the National Natural Science Foundation of China under Grant 61504112, Grant 11604285, and Grant 51605404, in part by the Technological Innovation Project of Economic and Information Commission of Fujian Province, in part by the Strait Postdoctoral Foundation of Fujian Province, in part by the Science and Technology Planning Project of Fujian Province under Grant 2018H6022, in part by the Natural Science Foundation of Fujian Province under Grant 2018J01103, and in part by the Science and Technology Project of Xiamen under Grant 3502Z20173016. Corresponding authors: Ziquan Guo and Zhong Chen (e-mail: zqguo@xmu.edu.cn; chenz@xmu.edu.cn).

Abstract: In this paper, we carry out the theoretical spectral optimization and perform experiments by varying temperature and electrical current primarily on one-phosphor-coated three-hump white light-emitting diode (LED) for healthy indoor or outdoor lighting by using the genetic algorithm (GA). White light with *low circadian action factor (CAF)* is propitious for bedroom lighting to help people relax and to promote sleep, whereas *high CAF* white light is beneficial for increasing working efficiency in the working place. We obtain low CAF or high CAF according to different application occasions (such as bedroom lighting or office lighting), good Commission Internationale de L'Eclairage color rendering index (R_a) or Illumination Engineering Society of North America color fidelity index (R_f), and color gamut index (R_g) or other color performances, and possibly high luminous efficacy of radiation (LER, K) at various correlated color temperatures (CCTs) from 2700 to 6500 K. For instance, in the case of one-phosphor-coated three-hump white LEDs at CCT = 3000 K, the low CAF as 0.264 ($R_a = 80$, $R_f = 77$, $R_g = 103$, and $K = 350.0$ lm/W) can be achieved, whereas that of standard light at the same CCT is 0.407. In addition, we also compare four types of three-hump white LEDs in performances of circadian action, luminous efficacy of radiation (LER), and color rendering. This paper can help both industry and academia understand the application of three-hump white LEDs in the healthy indoor or outdoor lighting.

Index Terms: Light-emitting diode, circadian action factor, color rendering index, color fidelity index, correlated color temperature.

1. Introduction

Light-emitting diodes (LEDs) have become promising lighting devices due to several well-known advantages, such as high luminous efficacy (LE), compact size, robustness, color-tunable property, environmental friendliness, and high reliability among others [1]. Currently, nitride-based white LEDs are manufactured by three common approaches [2]. 1) The yellow-green $Y_3Al_5O_{12}:Ce^{3+}$ ($YAG:Ce^{3+}$) phosphor is pumped by a blue LED chip (with the emission peak wavelength of 450 nm-460 nm), namely phosphor-coated (pc) white LEDs, 2) three monochromatic LED chips are combined with one another (RGB-LEDs), and 3) red, green, and blue phosphors are pumped by a near-ultraviolet LED or a violet LED (with the emission peak wavelength of 360 nm-410 nm). The most popular way generally belongs to the first category, owing to two primary advantages of (a) low cost compared with RGB-LEDs and (b) high LE compared with the third category. However, these LEDs generally suffer from high correlated color temperature (CCT) and low color rendering index (CRI, R_a) due to the lack of red light in the white light [3]. This problem of pc-white LEDs can be solved with a tunable color filter, but at the expense of decreased total light efficiency [4].

In recent decades, white LEDs have been optimized and designed for obtaining both high LE and high CRI by lowering LED's junction temperature [5], decreasing defect densities in the active region [6], roughening the surface [7], photon recycling [8], and spectral optimizing [9] among others. Among these technologies, the spectral optimizing technology is achieved by carefully tailoring the spectral shape of white LEDs to acquire both high CRI and high LE (or high luminous efficacy of radiation (LER, K)) simultaneously [9]. So far, researchers have carried out numerous theoretical and experimental studies on white LEDs in terms of CRI and LER [9]–[13]. For color rendering, although the CIE (Commission Internationale de L'Eclairage) CRI is the current standardized method, there are still some problems for its use in white LEDs [14]. As a consequence, IES (Illumination Engineering Society of North America) has adopted an alternative method (TM-30) which suggests two color indices (color fidelity index (CFI, R_f) and color gamut index (CGI, R_g)) for examining color properties [15]. Earlier, National Institute of Standards and Technology (NIST) has proposed another method called as color quality scale (CQS, Q_a) [14]. In addition to these spectral parameters, as a significant parameter related to both health and working efficiency, the circadian action factor (CAF) [16] proposed by Gall *et al.* [17] or the circadian stimulus (CS) proposed by Rea *et al.* [18] is frequently used to describe non-visual biological effects on humans (circadian effects). For human beings, the circadian effect is attributed to the third type of photoreceptors called as intrinsic photosensitive retinal ganglion cells (ipRGCs) [19]. These ipRGCs play key roles in the formation and release of melatonin, cortisol, and other hormones. Undergoing a significant circadian rhythm, the secretion of melatonin is suppressed during daytime, but becomes active at night. The white light with low CAF or low CS implies that less blue-rich light enters eyes, to decrease melatonin suppression and to help people relax at night in the bedroom; in contrast, high CAF or high CS means making people more exciting, thus increasing working efficiency in the daytime in the office or other working places [20]. Therefore, minimizing or maximizing CAF or CS constitutes an important task for the general healthy lighting. Recently in 2017, the Nobel Prize was awarded to scientists who studied biological clocks, and the healthy lighting has become increasingly important. Here, we primarily focus on studies of one-phosphor-coated three-hump white LEDs (or RG_pB-type LEDs), together with a comparison among four kinds of common three-hump white LEDs in consideration of circadian action, luminous efficacy of radiation, and color rendering.

2. Experimental Details for RG_pB-Type LEDs

In our previous works related to spectral optimization [12], [13], we have considered two important parameters as CRI and LER, but ignored the circadian rhythm. In this work, based on previously studied one-phosphor-coated three-hump white LEDs (blue LED chip (B)+yellow-green phosphor (G_p)+red LED chip (R), RG_pB-type LEDs, the subscript [p] denotes phosphor), we theoretically and experimentally studied their performances including circadian action, luminous efficacy of radiation, and color rendering. Here, although several available models, such as CS, are able to

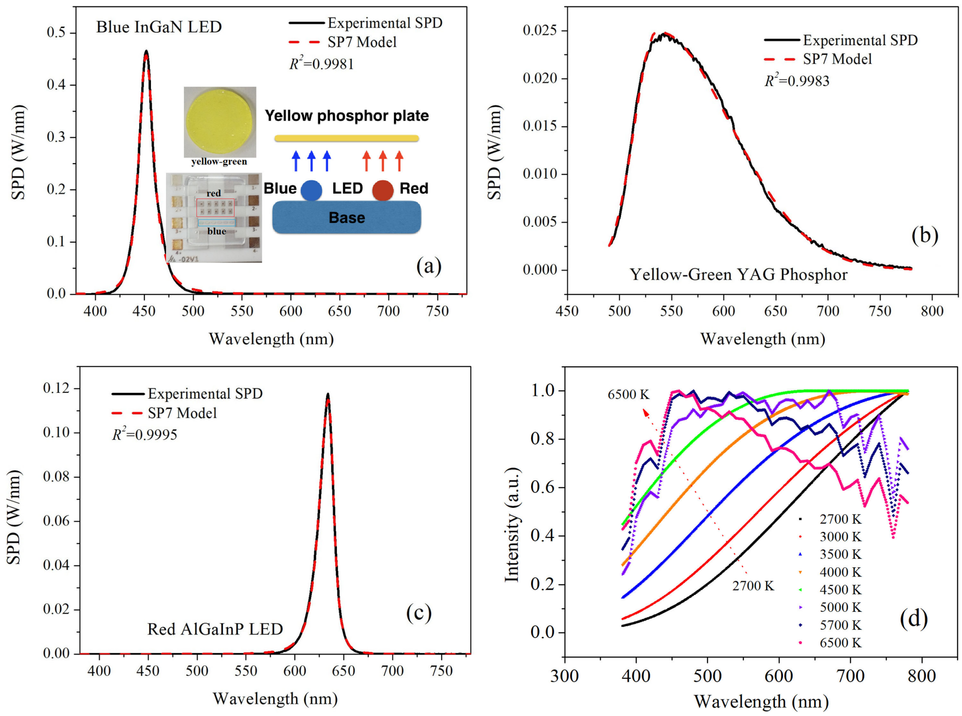

Fig. 1. Experimental SPDs and SP7 models for (a) blue InGaN-based LEDs, (b) yellow-green YAG-based phosphor plates, and (c) red AlGaInP-based LEDs. (d) The spectrum of standard light for eight CCTs. Inset of (a): the schematic structure of RG_pB-type three-hump white LEDs.

describe circadian action, we only employ the CAF for simplicity, which can be defined by the following equation [16]

$$CAF = \frac{K_c \int_{380\ \mathrm{nm}}^{780\ \mathrm{nm}} S_w(\lambda)C(\lambda)d\lambda}{K_m \int_{380\ \mathrm{nm}}^{780\ \mathrm{nm}} S_w(\lambda)V(\lambda)d\lambda} \tag{1}$$

where $C(\lambda)$ is the normalized circadian efficiency function (with the peak at around 450 nm) introduced by Gall *et al.*; the $V(\lambda)$ the normalized spectral luminous efficiency function (with the peak at about 555 nm); both curves are clearly illustrated in the literature [20]. K_c (blm/W) and K_m (683 lm/W) are the maximum value of the circadian efficiency function and the spectral luminous efficiency function, and are assumed to be equal to each other ($K_c = K_m$) in convenience [20]. We intend to compare the low CAF or high CAF of RG_pB-type LEDs with that of standard lights, so K_c value of 683 blm/W will not affect comparison results, whereas K_c is sometimes considered as 1817 blm/W in the literature [21]. The unit of CAF is blm/lm according to its definition in (1). In addition, the visual illuminance (VIL) of an artificial light source will affect the non-visual biological system [16], but we assume it as a constant value in this present work.

These studied one-phosphor-coated three-hump white LEDs are fabricated by *Xiamen Hualian Electronics Co. Ltd.*, schematically plotted in the inset of Fig. 1(a). They comprise blue InGaN-based LEDs containing six chips, yellow-green YAG-based remote phosphor plates, and red AlGaInP-based LEDs consisting of ten chips, and the white emission is finally the combination of blue, yellow-green, and red emission. This type of white LED is capable of offering extremely high CRI in excess of 95 at the CCT of 2000 K (the color of candle light) [12] to 6500 K (the color of sun light in the clear sky) [13]. In order to experimentally study circadian action of three-hump white LEDs, we carry out the following spectral measurement. During measurement, white LEDs are placed on a heat sink attached to a temperature controlling setup (Keithley-2510, Keithley Inc.)

TABLE 1
Fitting Coefficients in the SP7 Model

Coefficient	Blue LED	Yellow-Green phosphor	Red LED
a (nm)	8.757904	25.0106	11.09879
b	1.846829	-1.1607e+14	1.828542
c	1.306023	29.9896	1.804933

adjusted from 298 K to 338 K with an interval of 5 K, and are driven by two electrical source meters (Keithley-2400, Keithley Inc., and GS-610, Yokogawa Electric Corp.). Blue LEDs are direct-current (dc) driven at 100 mA by Keithley-2400; red LEDs are dc-supplied by GS-610 from 10 mA to 29 mA with an interval of 1 mA. Emission spectra of three-hump white LEDs are measured by using a 500 mm-diameter integrating sphere (ISP-500, Instrument Systems Inc.) connected to a spectrometer (Spectro-320e, Instrument Systems Inc.) after the operation of LEDs for more than 30 minutes, to guarantee that this measurement is under stable condition. Derived from the spectra, experimental peak wavelengths for blue, yellow-green, and red color component are approximately 451.7 nm (B), 535.4 nm (G_p), and 634.4 nm (R), respectively; experimental FWHMs for blue, yellow-green, and red color component are about 18.3 nm (B), 109.4 nm (G_p), and 17.3 nm (R), respectively. In the following optimization, we will adopt these FWHMs.

Prior to optimization, we need to generate the suitable mathematic model for RG_pB-type white LEDs firstly. The model used in our previous work [12] is more suitable for the simulation of spectra of RG_pB LEDs. In this mathematic model, the Split-PearsonVII function (SP7 model) is capable of precisely simulating spectra of blue LEDs, yellow-green phosphors, and red LEDs, as

$$P(\lambda, \lambda_{peak}, w) = \frac{1}{\left[1+\left(\frac{\lambda-\lambda_{peak}}{a}\right)^2\left(2^{\frac{1}{b}}-1\right)\right]^b}(\lambda < \lambda_{peak}); \frac{1}{\left[1+\left(\frac{\lambda-\lambda_{peak}}{w-a}\right)^2\left(2^{\frac{1}{c}}-1\right)\right]^c}(\lambda \geq \lambda_{peak}) \quad (2)$$

where λ is the emission wavelength; λ_{peak} the emission peak wavelength; w the full-width at half-maximum (FWHM); a, b, and c three fitting coefficients differed in various materials, like semiconductors and phosphors. Thus, the total model for white spectrum, $S_w(\lambda)$, is written as

$$S_w(\lambda) = H_bS_b(\lambda) + H_{gp}S_{gp}(\lambda) + H_rS_r(\lambda) \quad (3)$$

where $S_b(\lambda) = P(\lambda, \lambda_b, w_b)$, $S_{gp}(\lambda) = P(\lambda, \lambda_{gp}, w_{gp})$, and $S_r(\lambda) = P(\lambda, \lambda_r, w_r)$, are the normalized spectral power distribution (SPD) of the blue, yellow-green, and red color component, respectively; λ_b, λ_{gp}, and λ_r three peak wavelengths; H_b, H_{gp}, and H_r three relative peak heights; w_b, w_{gp}, and w_r three FWHMs. The comparisons between experimental SPDs and models are clearly observed in Figs. 1(a)–(c), with all coefficients of determination (R-square) in excess of 0.998, depicting considerably good agreements between these models and experimental SPDs. Table 1 lists fitting coefficients in SP7 models.

In this study, we carry out the optimization by treating yellow-green emission as independent emission, although in the real case, the yellow-green emission comes from down-converted silicate phosphors after absorbing certain proportions of blue light from InGaN-based LED chips. We also assume that the yellow-green phosphor does not absorb the red light, whose light energy is lower than the yellow-green one, for simplicity. For the realization of good color-rendering lighting, we primarily consider CIE CRI and set the limitation of CRI ($R_{a,o}$) as 80 (good color-rendering) and 90 (excellent color-rendering) in this section. We also calculate other indices including CIE R_9, IES R_f, IES R_g, and NIST Q_a. Referring to the CRI definition, the standard white light is regarded as Planckian Radiator for CCT $<$ 5000 K, while it is Standard Daylight for CCT $\geq$ 5000 K [22]. The studied CCT range is chosen as 2700 K-6500 K, corresponding to most CCTs of general white lighting. Fig. 1(d) shows the spectrum of standard light for eight studied CCTs. The CCT tolerance is regarded as 10 K, and the color distance (D_{uv}, in the CIE 1960 UCS color system) between calculated color coordinates of white LEDs and those of standard lights is kept within 0.01 (D_{uv} $\leq$ 0.01), to guarantee that calculated color coordinates are in accordance with those of standard

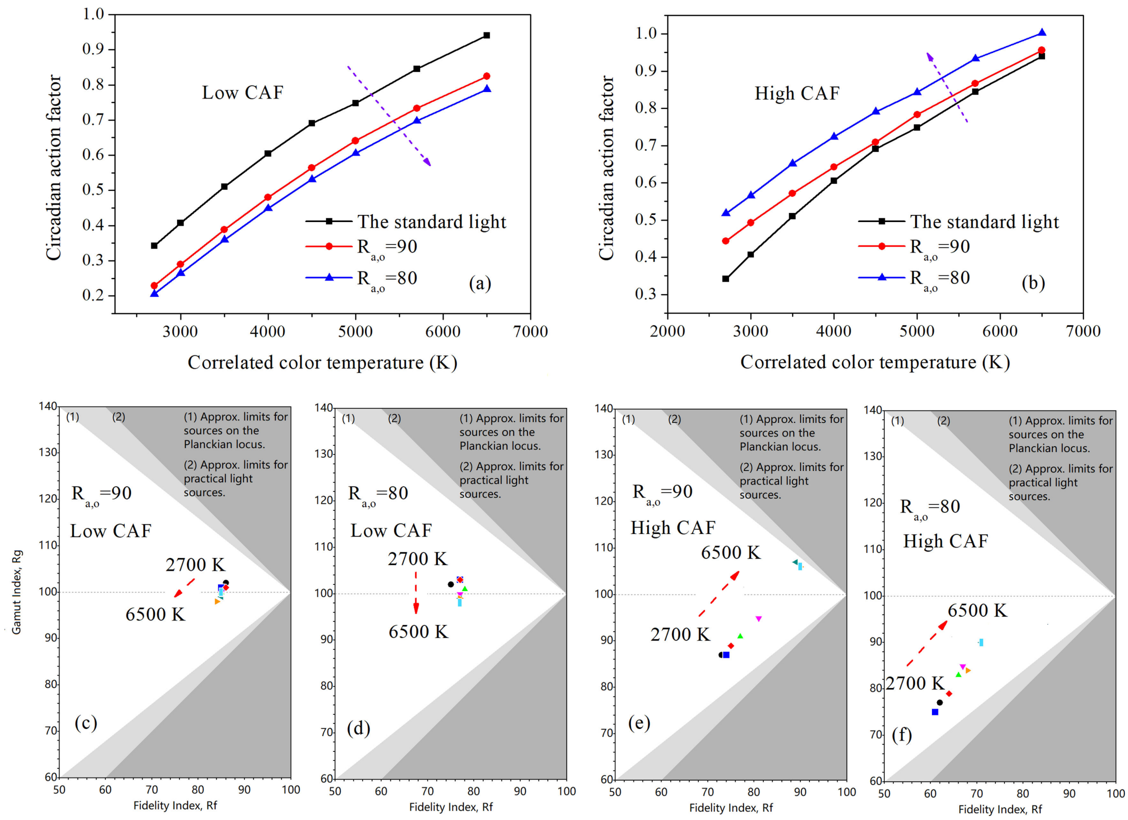

Fig. 2. (a) Low CAF and (b) high CAF of standard lights and white lights with $R_{a,o} = 80$ and 90 at eight representative CCTs as well as the IES R_f and R_g (c)–(f).

lights. We adopt the genetic algorithm (GA) optimization method and design a non-linear program by MATLAB software for achieving possibly minimum (*Min.*) or maximum (*Max.*) CAF value under eight specific CCT values. The GA method solves the optimization problem based on the biological evolution process. The objective function in GA is formulated as

$$F(\lambda_b, \lambda_{gp}, \lambda_r; w_b, w_{gp}, w_r; H_b, H_{gp}, H_r) = \text{Min.} \quad or \quad \text{Max.}\ CAF \tag{4}$$

During the optimization process, the peak wavelength range of blue, yellow-green, and red color component is set as 430 nm-490 nm (λ_b), 500 nm-590 nm (λ_{gp}), and 600 nm-670 nm (λ_r), respectively. Here, the FWHM values for three color components remain 18.3 nm (w_b), 109.4 nm (w_{gp}), and 17.3 nm (w_r), respectively.

3. Low or High Circadian Action for RG_pB-Type LEDs

3.1 Low or High CAF Versus High CRI for the Healthy Lighting

As mentioned previously, in some lighting fields, such as the bedroom lighting, it requires the white light with low circadian action to help people relax and to promote sleep; in contrast, for office lighting, it requires the high circadian action white light for increasing working efficiency. Of course, both applications need sufficiently high color rendering at the same time. Here, we present a set of calculated results with low CAF or high CAF and high color rendering metrics along with possibly high LER, and carry out following analyses. As can be observed in Figs. 2(a) and (b), as the CCT increases (or decreases), the minimum or maximum CAF at each CCT increases (or decreases), too. It is obviously that the CAF will decrease by reducing the blue content of white light due to

TABLE 2
A Set of Optimal (Low or High) CAFs and CAF Differences at Eight Representative CCTs of 2700 K–6500 K

CCT(K)	2700	3000	3500	4000	4500	5000	5700	6500
CAF_s	0.342	0.407	0.510	0.605	0.691	0.748	0.845	0.940
low-CAF_w, $R_{a,o}$=80	0.205	0.264	0.360	0.449	0.531	0.606	0.697	0.787
Δ(%), $R_{a,o}$=80	-39.9	-35.1	-29.5	-25.8	-23.1	-19.0	-17.5	-16.3
low-CAF_w, $R_{a,o}$=90	0.229	0.290	0.389	0.480	0.564	0.641	0.733	0.825
Δ(%), $R_{a,o}$=90	-33.1	-28.8	-23.8	-20.6	-18.3	-14.3	-13.2	-12.3
high-CAF_w, $R_{a,o}$=80	0.518	0.566	0.651	0.723	0.791	0.843	0.933	1.002
Δ(%), $R_{a,o}$=80	+51.5	+39.0	+27.7	+19.6	+14.4	+12.7	+10.4	+6.6
high-CAF_w, $R_{a,o}$=90	0.444	0.493	0.572	0.643	0.709	0.783	0.867	0.956
Δ(%), $R_{a,o}$=90	+29.7	+21.1	+12.1	+6.2	+2.6	+4.7	+2.6	+1.7

the overlapping of circadian efficiency curve and blue spectrum, corresponding to decreasing CCT. From Figs. 2(a) and (b), we also observe that CAFs at various CCTs for $R_{a,o} = 80$ are lower or higher than those for $R_{a,o} = 90$. To quantify it, we then calculate the difference of CAF between standard lights and white LEDs at $R_{a,o} = 80$ and 90, respectively. The difference of CAF is defined as,

$$\Delta = \frac{CAF_w - CAF_s}{CAF_s}(\%) \tag{5}$$

where CAF_w represents the CAF of white LED light; CAF_s the CAF of standard light. The CAF differences are listed in Table 2 in detail. In comparison of white light at $R_{a,o} = 90$ and standard light, a maximum CAF decrease of 33.1% at 2700 K CCT (average of 20.5% for 2700 K-6500 K CCTs) can be observed, while for $R_{a,o} = 80$, a maximum decrease of 39.9% at 2700 K CCT (average of 25.8% for 2700 K-6500 K CCTs) can be found. In the high CAF case, in comparison of white light at $R_{a,o} = 90$ and standard light, a maximum CAF increase of 29.7% at 2700 K CCT (average of 10.1% for 2700 K-6500 K CCTs) can be observed, while in the case of $R_{a,o} = 80$, a maximum increase of 51.5% at 2700 K CCT (average of 22.8% for 2700 K-6500 K CCTs) can be noticed. Both phenomena indicate that more CAF decreases or increases happen at lower CCTs, and it seems more applicable to achieve lower or higher CAFs at a CRI of around 80 than 90. One point we are desired to emphasize is that, if FWHMs of chips and phosphors are not fixed at specific values together with improved optimization methods used, calculated CAFs under identical conditions may become much lower or higher than those presented in Table 2. In this calculation, we treat CRI as the primary color rendering metric, so the calculated R_f and R_g are not sufficiently high, especially for high-CAF case (seen in Figs. 2(c)–(f)). Further works would treat the IES TM-30 as main method. In the real case, people would prefer to low-CCT white LEDs for bedroom lighting and high-CCT white LEDs for office lighting. The purpose of minimizing or maximizing CAF for all CCTs of 2700 K-6500 K in this work is to comprehensively understand the CAF difference between white LEDs and standard ones. In the following comparison among four types of three-hump white LEDs, we will only consider a low CCT (3000 K) for bedroom lighting and a high CCT (6500 K) for office lighting more practically.

3.2 Current and Temperature Dependencies of Circadian Action and Color Rendering

Fig. 3(a) shows CAF and CRI as a function of electrical current of red LEDs. As current increases, the CRI increases first and is peaked at 23 mA, and then decreases. The CAF decreases as the current increases. The change of CRI and CAF is corresponding to the spectral variation of red color component, as shown in Fig. 3(b). Compared with the standard light at a CCT of 4000 K (CAF = 0.605), the experimental CAF difference is only -3.9 % (CAF = 0.581, 20 mA electrical current of red LEDs, 4011 K CCT, 90 CRI). The color rendering is excellent for these LEDs, but circadian action is possibly limited by the wavelength combination of three spectral humps. Fig. 3(d)

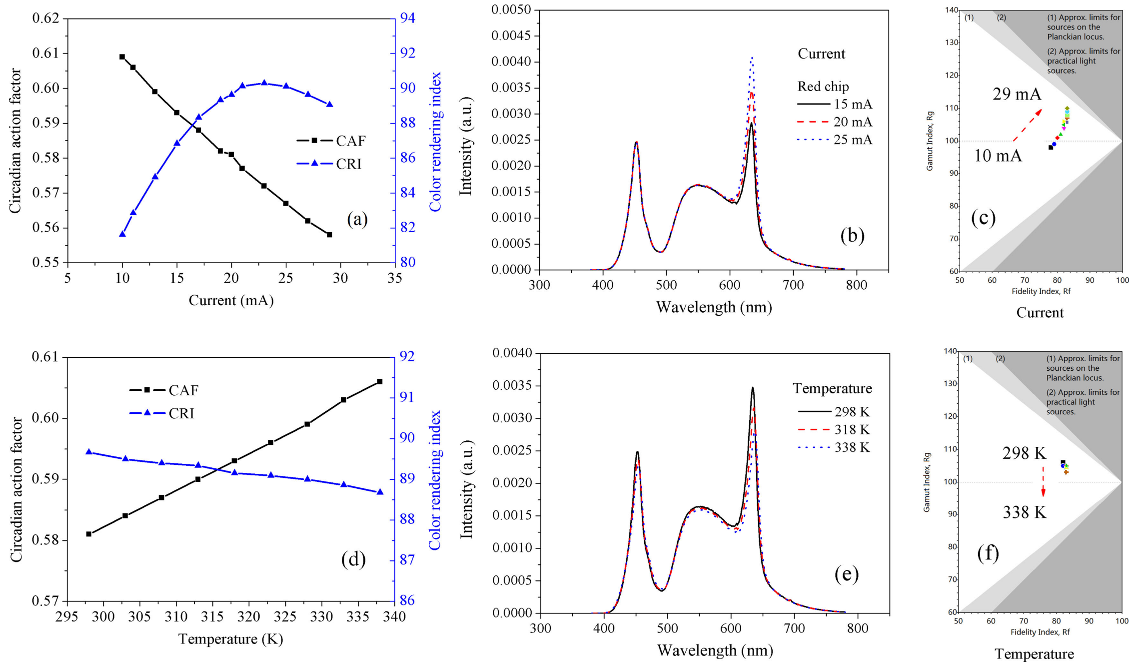

Fig. 3. (a) CAF and CRI versus electrical current. (b) Spectral variation with the change of electrical current. (c) R_f and R_g versus electrical current. (d) CAF and CRI versus temperature. (e) Spectral variation with the change of temperature. (f) R_f and R_g versus temperature. Here, the electrical current represents that of red LEDs.

shows the CAF and CRI as a function of temperature. From 298 K to 338 K, the temperature induces the increase of circadian action from 0.581 to 0.606, but the CRI decreases slightly. From Fig. 3(e), we notice that the blue and red emissions decrease as the heat-sink temperature increases, whereas the yellow emission changes slightly, owing to good thermal stabilities of YAG phosphor. In particular, the decrease of red emission is more remarkable than blue one, making the spectral barycenter slightly shift to maximum value of circadian efficiency curve and leading to high CAF. The current- and temperature-dependent IES R_f and IES R_g are also plotted in Figs. 3(c) and (f). In the actual application, both circadian action and color rendering of three-hump white LEDs will be affected by the ambient temperature, especially for the outdoor lighting, whose temperature varies largely by the external environment. Therefore, for solving those issues, the well design of inverse-feedback drive circuits and thermal dissipation tunnels for optical stabilities is of great importance.

4. A Theoretical Comparison Among Four Kinds of White LEDs

In addition to RG_pB-type LED (one-phosphor), there are other three types of three-hump white LEDs, such as 1) white LEDs combing red, green, and blue chips (RGB-type LED, non-phosphor), 2) yellow-green and red phosphors pumped by blue LEDs (R_pG_pB-type LED, two-phosphor), 3) blue, green, and red phosphors pumped by near-ultraviolet LEDs ($R_pG_pB_p$-type LED, three-phosphor). For R_pG_pB-type LED, for example, the yellow-green phosphor can be chosen as YAG:Ce^{3+} phosphor or other yellow-green phosphors (e.g. β-sialon:Eu^{2+}) [23]. The red phosphor may be K_2SiF_6:Mn^{4+} or $CaAlSiN_3$:Eu^{2+} [23]. In addition to rare-earth phosphors, the down-conversion materials in above phosphor-type white LEDs can be nanocrystal quantum dots (QDs), including CdSe/ZnS QDs [10] and Perovskite QDs [24]. The community may be interested in the problem which type of three-hump white LED performs the best in terms of color rendering, luminous ef-

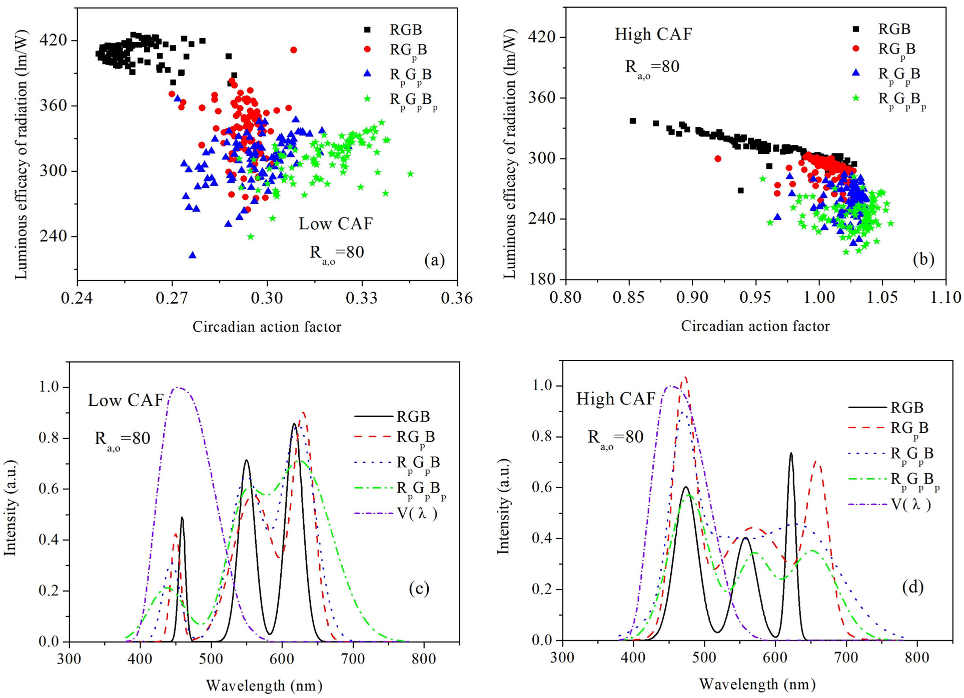

Fig. 4. (a) Low CAF and (b) high CAF versus LER for four types of white LEDs at $R_{a,o} = 80$. Optimal spectrum for (c) low CAF and (d) high CAF at $R_{a,o} = 80$.

ficacy of radiation, and circadian action. Therefore, authors are desired to conduct a comparing investigation on these four types of white LEDs. For color rendering, we also consider the CRI as the primary parameter, with IES R_f, IES R_g, NIST Q_a, and CIE R_9 as the supplement. For the spectral modeling, emission spectra of various types of phosphors or LEDs are very different, and coefficients presented in Table 1 are only suitable for YAG phosphor, InGaN blue LED, and AlGaInP red LED. Determining all coefficients of other phosphors and LEDs is cumbersome. Therefore, we use a simple Gaussian Model [9], [10] instead in this section. FWHMs of 10 nm-40 nm are for chips and QDs [10], [24]; FWHMs of 50 nm-130 nm belong to rare-earth phosphors [13], [23]. For $R_pG_pB_p$-type LED, although a small part of violet or ultra-violet emission (360 nm-410 nm) may contribute to the total white emission in the visible region (380 nm-780 nm), we neglect this contribution in the simulation by assuming that violet or ultra-violet emission is all absorbed by phosphors. For low CAF, we consider the CCT of 3000 K close to Standard A light source (2856 K), which is more suitable for bedroom lighting, while for high CAF, the CCT of 6500 K close to sun light of D65 is more suitable for office lighting. Figs. 4(a) and (b) depict many calculated CAFs versus LERs for four types of white LEDs at a fixed CRI of 80, sufficient for most of lighting occasions. Due to the fact that the general GA is possibly limited by its own algorithm which can only achieve local optimum values, these points in figures represent many sub-optimal results by multiple general-GA calculations, to make a more abundant comparison. Among four types, RGB-type LEDs perform the best in the achievement of both high LER and low CAF at $R_{a,o} = 80$. For obtaining high CAF, $R_pG_pB_p$-type LEDs have shown the best performance, but with lowest luminous efficacy. RG_pB-type and R_pG_pB-type LEDs exhibit a nearly identical behavior in low or high CAF, but luminous property is better for the former than the latter. Since RGB-type LEDs have highest cost and complicated drive system as well as relatively low color rendering properties, $R_pG_pB_p$-type and R_pG_pB-type LEDs own lowest luminous efficacy due to lowest LER and most Stokes losses due to multiple optical excitation process among different materials of phosphor, one-phosphor-coated white LEDs seem to be the best choice for general healthy lighting among four solutions. Table 3 listed a set of

TABLE 3
The Optimal CAF, CAF Difference, D_{uv}, K, CIE R_a, CIE R_9, IES R_f, IES R_g, and NIST Q_a of Four-Type Three-Hump White LEDs Under Two CCTs

Low CAF (3000 K)	CAF_w	Δ(%)	R_a	R_9	Q_a	R_f	R_g	K (lm/W)	D_{uv}
RGB	0.247	-39.4	80	53	63	69	101	407.9	0.0054
RG_pB	0.270	-33.7	80	76	70	75	103	371.1	0.0054
R_pG_pB	0.272	-33.2	80	50	72	74	104	366.5	0.0054
$R_pG_pB_p$	0.291	-28.5	80	42	72	77	100	311.4	0.0054
High CAF (6500 K)	CAF_w	Δ(%)	R_a	R_9	Q_a	R_f	R_g	K (lm/W)	D_{uv}
RGB	1.028	9.3	80	30	74	68	85	294.4	0.0054
RG_pB	1.033	9.9	80	44	83	73	90	245.2	0.0047
R_pG_pB	1.038	10.4	80	43	85	79	96	235.5	0.0054
$R_pG_pB_p$	1.056	12.4	80	44	84	78	94	235.7	0.0054

optimal (best) CAFs and relevant calculated parameters for four types of LEDs, with optimal spectra illustrated in Figs. 4(c) and (d), respectively.

5. Conclusion

In summary, we have carried out theoretical spectral optimizations and experiments for three-hump white LEDs in terms of circadian action (CAF), color rendering indices (including CIE R_a, CIE R_9, IES R_f, IES R_g, and NIST Q_a), and possibly high LER at eight CCTs. During the optimization, the general GA has been used to solve the problem of achieving the minimum or maximum CAF while meeting certain conditions. Results show the averaged CAF decrease of 25.8% ($R_{a,o} = 80$) and increase of 22.8% ($R_{a,o} = 80$) under eight CCTs in comparison with the CAF of standard lights. The optimal CAF for $R_{a,o} = 80$ is lower or higher than that for $R_{a,o} = 90$ at each CCT from 2700 K to 6500 K, indicating that the white light with $R_{a,o} = 80$ appears to be more beneficial for the bedroom lighting (using low-CAF white LEDs) or the office lighting (using high-CAF white LEDs) than that with $R_{a,o} = 90$, implying that lower-CRI white lights show much larger CAF adjustable space. Additionally, we theoretically compare four types of three-hump white LEDs, including non-phosphor, one-phosphor, two-phosphor, and three-phosphor white LEDs. Therefore, we conclude that studied three-hump phosphor-coated white LEDs, especially one-phosphor-coated white LEDs, are regarded as potential candidates for healthy indoor or outdoor lighting.

Acknowledgment

The authors would like to thank the anonymous reviewers for their valuable suggestions. The first author would like to thank his newborn baby, Lingxi Guo (Xiao Maoxian), for arriving in this world in September 2018 and bringing him tremendous joy.

References

[1] E. F. Schubert and J. K. Kim, “Solid-state light sources getting smart,” *Science*, vol. 308, no. 5726, pp. 1274–1278, May 2005.
[2] C. K. Tan and N. Tansu, “Nanostructured lasers: Electrons and holes get closer,” *Nature Nanotechnol.*, vol. 10, no. 2, pp. 107–109, Feb. 2015.
[3] T. Wu *et al.*, “Mini-LED and micro-LED: Promising candidates for the next generation display technology,” *Appl. Sci.-Basel*, vol. 8, no. 9, Sep. 2018, Art. no. 1557.
[4] Z. He, H. Chen, Y. Lee, and S. Wu, “Tuning the correlated color temperature of white light-emitting diodes resembling Planckian locus,” *Opt. Exp.*, vol. 26, no. 2, pp. A136–A143, Jan. 2018.
[5] H. Chen, S. Lin, and C. Xiong, “Analysis and modeling of thermal effect and optical characteristic of LED systems with parallel plate-fin heatsink,” *IEEE Photon. J.*, vol. 9, no. 2, Apr. 2017, Art. no. 8200411.
[6] Y. Lin *et al.*, “Evolution of crystal imperfections during current-stress ageing tests of green InGaN light-emitting diodes,” *Appl. Phys. Exp.*, vol. 9, no. 9, Sep. 2016, Art. no. 092101.
[7] T. W. Kuo, S. X. Lin, Y. Y. Hung, J. H. Horng, and M. P. Houng, “Improved extraction efficiency of light-emitting diodes by wet-etching modifying AZO surface roughness,” *IEEE Photon. Technol. Lett.*, vol. 23, no. 6, pp. 362–364, Mar. 2011.

[8] A. I. Zhmakin, "Enhancement of light extraction from light emitting diodes," *Phys. Rep.*, vol. 498, no. 4/5, pp. 189–241, Feb. 2011.
[9] A. Žukauskas, R. Vaicekauskas, F. Ivanauskas, R. Gaska, and M. S. Shur, "Optimization of white polychromatic semiconductor lamps," *Appl. Phys. Lett.*, vol. 80, no. 2, pp. 234–236, Jan. 2002.
[10] T. Erdem, S. Nizamoglu, X. W. Sun, and H. V. Demir, "A photometric investigation of ultra-efficient LEDs with high color rendering index and high luminous efficacy employing nanocrystal quantum dot luminophores," *Opt. Exp.*, vol. 18, no. 1, pp. 340–347, Jan. 2010.
[11] J. J. Zhang, R. Hu, X. J. Yu, B. Xie, and X. B. Luo, "Spectral optimization based simultaneously on color-rendering index and color quality scale for white LED illumination," *Opt. Laser Technol.*, vol. 88, pp. 161–165, Feb. 2017.
[12] Z. Guo, H. Lu, T. Shih, Y. Lin, Y. Lu, and Z. Chen, "Spectral optimization of candle-like white light-emitting diodes with high color rendering index and luminous efficacy," *IEEE/OSA J. Display Technol.*, vol. 12, no. 11, pp. 1393–1397, Nov. 2016.
[13] Z. Guo *et al.*, "Optimization studies of two-phosphor-coated white light-emitting diodes," *IEEE Photon. J.*, vol. 5, no. 2, Apr. 2013, Art. no. 8200112.
[14] W. Davis and Y. Ohno, "Color quality scale," *Opt. Eng.*, vol. 49, no. 3, Mar. 2010, Art. no. 033602.
[15] Illuminating Engineering Society of North America, *IES Method for Evaluating Light Source Color Rendition*. New York, NY, USA: Illuminating Eng. Soc., 2015.
[16] J. H. Oh, S. J. Yang, and Y. R. Do, "Healthy, natural, efficient and tunable lighting: four-package white LED for optimizing the circadian effect, color quality and vision performance," *Light Sci. Appl.*, vol. 3, no. 2, pp. 1–9, Feb. 2014.
[17] D. Gall and K. Bieske, "Definition and measurement of circadian radiometric quantities," in *Proc. CIE Symp.*, 2004, pp. 129–132.
[18] M. S. Rea, M. G. Figueiro, A. Bierman, and R. Hamner, "Modelling the spectral sensitivity of the human circadian system," *Lighting Res. Technol.*, vol. 44, no. 4, pp. 386–396, 2012.
[19] D. M. Berson, F. A. Dunn, and M. Takao, "Phototransduction by retinal ganglion cells that set the circadian clock," *Science*, vol. 295, no. 5557, pp. 1070–1073, Feb. 2002.
[20] T. Wu *et al.*, "Multi-function indoor light sources based on light-emitting diodes–A solution for healthy lighting," *Opt. Exp.*, vol. 24, no. 21, pp. 24401–24412, Oct. 2016.
[21] A. Zabiliūtė, R. Vaicekauskas, P. Vitta, and A. Žukauskas, "Phosphor-converted LEDs with low circadian action for outdoor lighting," *Opt. Lett.*, vol. 39, no. 3, pp. 563–566, Feb. 2014.
[22] Technical Committee 1-62, "Color rendering of white LED light sources," CIE, Vienna, Austria, Tech. Rep. CIE 177:2007, 2007.
[23] P. F. Smet, A. B. Parmentier, and D. Poelman, "Selecting conversion phosphors for white light-emitting diodes," *J. Electrochem. Soc.*, vol. 158, no. 6, pp. R37–R54, 2011.
[24] Y. Li *et al.*, "One-step preparation of long-term stable and flexible $CsPbBr_3$ perovskite quantum dots/ethylene vinyl acetate copolymer composite films for white light-emitting diodes," *ACS Appl. Mater. Interfaces*, vol. 10, no. 18, pp. 15888–15894, May 2018.